EUROPEAN COOPERATION
IN THE FIELD OF SCIENTIFIC
AND TECHNICAL RESEARCH

EURO-COST

COST 273 TD(02)027
Guildford, UK
January 17-18, 2002

SOURCE: Centre for Communications Research, University of Bristol, UK.
Telia Research AB, Malmö, Sweden.
Allgon Systems AB, Täby, Sweden.

Frequency Dependency of the Spatial-Temporal Characteristics of UMTS FDD Links

S E Foo[1], M A Beach[1], P Karlsson[2], P Eneroth[2], B Lindmark[3] and J Johansson[3]

[1] University of Bristol,
Queen's Building,
University Walk, Clifton,
Bristol BS8 1TR,
UK.
Phone: +44 117 928 8617
Fax: +44 117 954 5206
Email: S.E.Foo@bristol.ac.uk
M.A.Beach@bristol.ac.uk

[2] Telia Research AB,
Box 94,
SE-201 20 Malmö,
Sweden.
Phone: +46 40 10 51 77
Fax: +46 40 30 70 29
Email: Peter.C.Karlsson@telia.se
Peter.B.Eneroth@telia.se

[3] Allgon Systems AB,
Antennvägen 6,
187 80 Täby,
Sweden.
Phone: +46 8 540 826 39
Fax: +46 8 540 834 80
Email: Bjorn.Lindmark@allgon.se
Jonny.Johansson@allgon.se

FREQUENCY DEPENDENCY OF THE SPATIAL-TEMPORAL CHARACTERISTICS OF UMTS FDD LINKS

S E Foo[1], M A Beach[1], P Karlsson[2], P Eneroth[2], B Lindmark[3] and J Johansson[3]

[1]University of Bristol, UK
[2]Telia Research AB, Sweden
[3]Allgon Systems AB, Sweden

ABSTRACT

Smart antennas promise to provide range extension and capacity enhancements crucial to the successful deployment of Universal Mobile Telecommunications System (UMTS) networks. The frequency offset between the uplink and downlink in the Frequency Division Duplex (FDD) air interface gives rise to a frequency dependency in the channel responses and potential problems in downlink beamforming. In order to investigate this, a highly novel dual-band, dual-polarised channel sounding trial was performed in the UMTS FDD bands by the University of Bristol. The wideband measurements were conducted in the City of Bristol, encompassing urban city and sub-urban residential scenarios and subsequent post processing was performed to extract channel parameters across the two bands.

This paper presents the results and analysis done so far. It was observed that there was generally a higher degree of scattering in the higher frequency band, resulting in larger angular spreads and delay spreads in most locations. The channels also exhibited a strong degree of de-correlation when viewed from the spatial and temporal domains.

1 INTRODUCTION

Smart antennas are crucial to the successful deployment of UMTS networks as they offer range extension and capacity enhancement via spatial processing of the received signal vector [1]. However, in the UMTS Terrestrial Radio Air-interface (UTRA) FDD, there is a 190MHz separation between the uplink and the downlink [2]. Downlink beamforming schemes based on channel estimation done in the uplink assumes a degree of correlation between these two channels. There is therefore a need to quantify the degree of correlation between these two channels such that accurate channel models may be described and to develop robust downlink beamforming schemes. Previous trials conducted in Bristol were performed with a frequency separation of only 15MHz [3,4], this paper reports a much enhanced equipment facility supporting a 200MHz separation, which is more representative of the UTRA FDD network deployment.

In Section 2, the measurement equipment along with the customisations performed for dual band channel sounding are described. Section 3 presents the measurement campaign, where the location and the measurement format are described. Post processing analysis of the measured data is presented in Section 4, together with various extracted channel parameters. Finally, Section 5 presents the conclusions and suggestions for future work.

2 MEASUREMENT EQUIPMENT

The basis for the measurement system was the state-of-the-art Medav RUSK BRI channel sounder [5]. In its standard form, the Medav channel sounder transmits with a centre frequency in the range of 1.8GHz-2.5GHz, selectable in 100MHz steps and with a maximum bandwidth of 120MHz as well as offering a 5.2GHz capability.

The aim of the customisation was to enable the transmitter to transmit two simultaneous bands of signals at 1.91GHz-1.93GHz and 2.11GHz-2.13GHz. This resulted in a Tx Chassis (Figure 1) which performs the up-conversion to the 2.1GHz band with the Medav set to transmit at the 1.9GHz band. The signal levels between the two bands were carefully balanced to within 1dB of each other before being fed to dedicated power amplifiers. The outputs from these were then combined via a diplexer resulting in a total power of +40dBm in each band. A 2dBi gain omni-directional sleeve dipole antenna was mounted in a slant 45° position on the vehicle roof to excite the mobile channel.

At the receiving end, a custom made 8-element ±45° polarisation UMTS array was provided by Allgon Systems AB (Figure 2). Each sub-array was a panel array with fixed weighting providing a 3dB azimuth beamwidth of approximately 100° and about 15dBi of gain. Further, an electrical downtilt of about 2° was also applied and the panels were spaced apart 80mm in a linear uniform array format. The array was calibrated in an anechoic chamber in order to generate a correction matrix which ensured minimal mutual coupling between the elements [6], thus ensuring accurate subsequent Direction of Arrival (DOA) estimation. The calibration

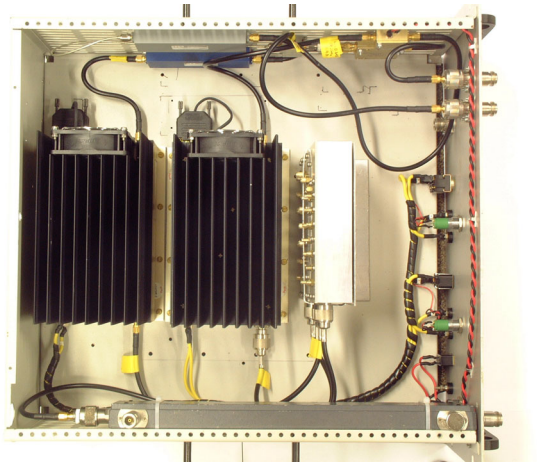

Figure 1: Tx Chassis

Figure 2: Allgon array

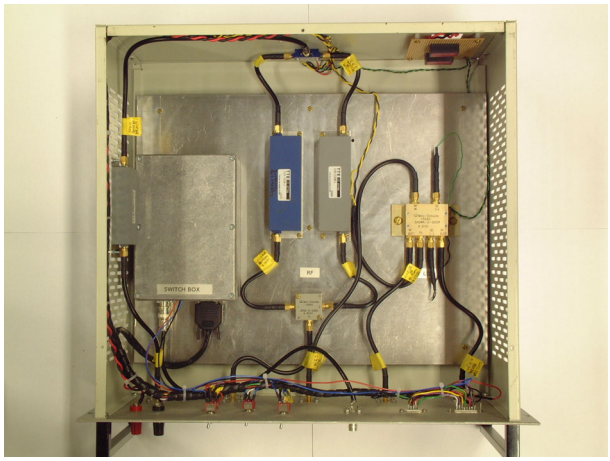

Figure 3: Rx Chassis

was performed at the 1.9GHz and 2.1GHz bands since the array separation of 80mm resulted in different wavelength spacings at the two frequency bands.

An array back plate was mounted to the back of the array. This contained 8 2:1 polarisation switches as well as an 8:1 multiplexer to switch the correct element sequentially thus multiplexing the 16 ports into a single output. An array box was designed to control the switching operations and to ensure that the correct element was selected in synchronisation with the receiver.

An Rx Chassis (Figure 3) was built to sequentially switch between the two bands and polarisations, as described in Section 3. Essentially, the receiver was time multiplexed between the antenna elements, frequency bands and polarisations to enable the measurements to be done in pseudo real time. The Rx Chassis routes the signal from the array to the correct bandpass filter (1.9GHz or 2.1GHz) and also switches between an external signal generator and Medav's own internal LO, which has been cabled out from the receiver. With the Medav receiver set to receive at 1.9GHz, the external signal generator was set at 200MHz higher than Medav's internal Local Oscillator (LO) frequency for the 2.1GHz band signals. The correct LO signal is then fed into the Medav receiver's mixer such that the resulting Intermediate Frequency (IF) will always be correct regardless of the incoming signal band. The measured data files are then de-interleaved according to their frequency and polarisation during post processing.

All the external signal generators were phase referenced to the 10MHz Medav rubidium clocks. The clocks were allowed to warm up and stabilise before measurements were performed to ensure minimal drift and optimum phase stability which is crucial in preserving the accuracy of the time of flight and integrity of the measured channel phase relationships.

A GPS receiver was also employed to produce location information by having its data logged into a laptop. The clock on the laptop and the Medav receiver was synchronised to the Coordinated Universal Time (UTC) as shown by the GPS receiver. This is to enable a time stamp of the location and measurement data which allows the exact location during a measurement to be traced back during post processing.

Finally, a back to back system calibration was performed before the start of the measurements to remove the time delay induced by the components as well as its amplitude response. This ensures that the absolute time of flight and path loss of the channel is measured, with all contributions due to the measurement system calibrated out.

3 MEASUREMENT CAMPAIGN

The system was setup to measure a snapshot of 8 Complex Impulse Responses (CIRs) across the array for each frequency band and polarisation. A measurement period (excess delay) of 6.4μs was chosen as it allows a total round trip signal path of up to about 2km, which is suitable for the channel measured. Since each CIR takes 12.8μs (6.4μs to measure and 6.4μs to perform

switching), a complete snapshot takes 102.4μs. This was done sequentially and back to back such that a total of 32 snapshots (8 for each band and polarisation combination) were recorded and this makes one Fast Doppler Block (FDB). The system then pauses for 40.96ms before repeating this process again. The sequence used in the measurement was 2.1GHz +45° Polarisation, 1.9GHz +45° Polarisation, 2.1GHz -45° Polarisation and 1.9GHz -45° Polarisation.

2 scenarios were measured, Triangle which is an urban city setting (cluttered small urban cell) and Redland, which is a sub-urban residential environment. 2 kinds of measurements were performed, static where the transmitter would be parked at pre-defined locations whilst measurements were collected, and dynamic where a drive route was performed with the receiver recording data throughout the route. 12 static locations were chosen for each environment, and in addition, 3 drive routes for the Triangle measurements (Figure 4) and 2 drive routes for the Redland measurements (Figure 5).

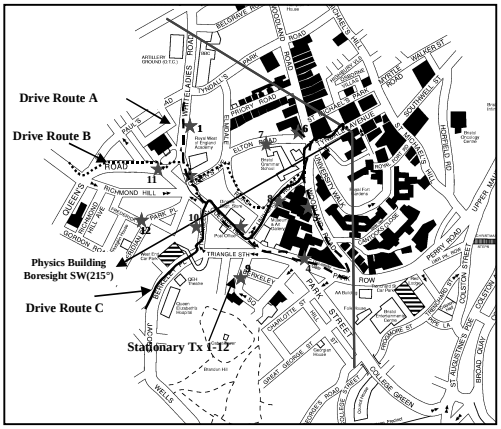

Figure 4: Triangle Urban Area

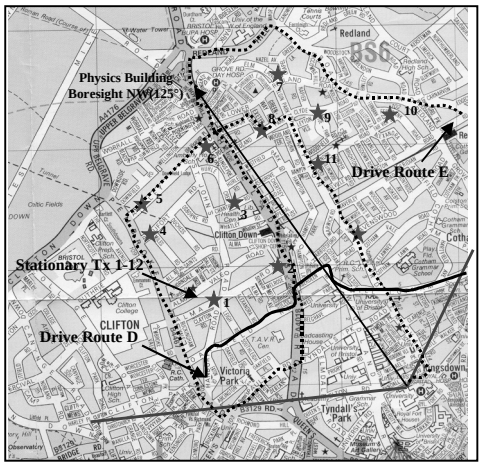

Figure 5: Redland Sub-Urban Area

This paper describes the post processing done for the +45° Polarisation static measurements.

The receiving array was mounted on the roof of the Physics Building, which is 30m above ground level and provided good aerial view of the 2 scenarios. For the Triangle measurements, the array was pointed South-West (215°) and North-West (305°) for the Redland measurements. The array was mounted about 3.5m from the floor of the roof and given an additional mechanical downtilt of 4°, thus giving a total downtilt of 6°.

4 DATA ANALYSIS

The measured data was in the form of complex frequency response with a bandwidth of 20MHz for each frequency band. A 2D Unitary ESPRIT [7] super-resolution algorithm was employed to estimate the multipath components' time of arrival, direction of arrival and power. A 15dB threshold was applied where multipath components of power more than 15dB below the most powerful component were rejected as noise. 8 successive snapshots for each frequency band and polarisation combination were used for each estimation to provide averaging. The 8 snapshots are statistically similar as they were measured in less than 3.3ms, which is below the coherence time of the channel. 400 snapshots were used in blocks of 8 snapshots in the estimation for each combination of band and polarisation, giving 50 estimates of each channel over a period of about 2.2s. Table 1 shows the parameters extracted for the +45° Polarisation view of the 1.9GHz and 2.1GHz channel. These parameters have been averaged over the 2.2s time period and over all 12 locations for each scenario.

Parameters	Triangle		Redland	
	1.9GHz	2.1GHz	1.9GHz	2.1GHz
$\tau_{RMS}/\mu s$	0.133	0.129	0.114	0.135
$\varphi_{RMS}/^{\circ}$	8.4	9.6	3.1	6.2
B_{COH}/MHz	1.00	0.943	1.29	0.842
n	3.28	3.21	3.26	3.27
$\rho_{TEMPORAL}$	0.33		0.35	
$\rho_{SPATIAL}$	0.12		0.20	

Table 1: Extracted Channel Parameters for +45° Polarisation

The RMS delay spread, τ_{RMS} was evaluated and Figure 6 shows the averaged RMS delay spread over 2.2s for each location, scenario and frequency band.

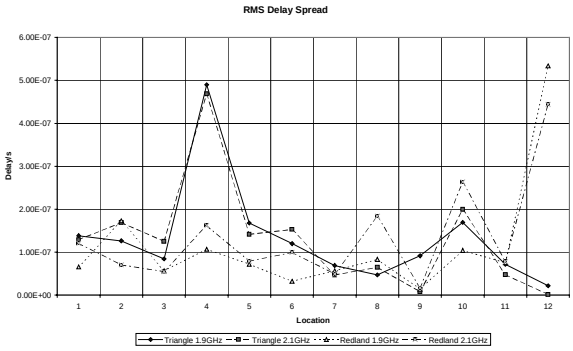

Figure 6: RMS Delay Spread for +45° Polarisation

It can be seen that the 2.1GHz channel generally exhibits higher RMS delay spreads compared to the 1.9GHz channel for both scenarios. The Triangle environment also shows higher spreads which is expected as it is a more cluttered urban environment. Triangle's Location 4 has a high RMS delay spread as it is down in a street canyon where most of the received rays were reflected and diffracted over the roofs of the shop lots along that street. Redland's Location 12 also shows high RMS delay spread and is due to the hilly environment in that area which results in multipath scattering and is reflected in the impulse response.

The RMS azimuth spread, φ_{RMS} was evaluated with a similar equation for RMS delay spread but φ_k, the angle of arrival of the k'th multipath component was used in the evaluation instead [8,9,10]. Figure 7 shows a similar graph to Figure 7 but is viewed from the spatial domain which is the RMS azimuth spread.

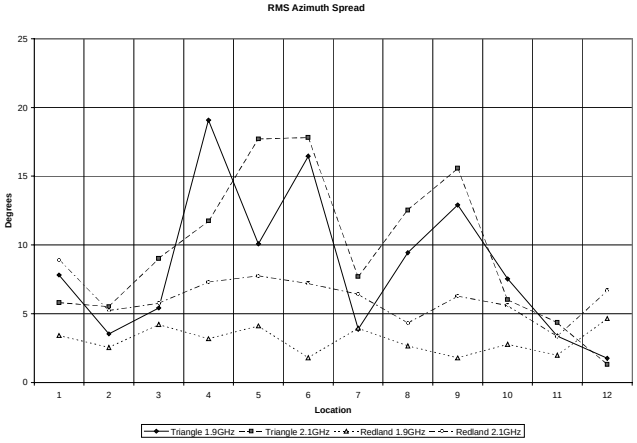

Figure 7: RMS Azimuth Spread for +45° Polarisation

The trend exhibits generally higher scattering at the higher frequency band for both scenarios which is consistent with the observation in the temporal domain. Triangle's Location 4 shows a high degree of azimuth spread, confirming its multipath rich propagation. Triangle's Location 5 and 9 is along a steep incline and this causes ground induced echoing as was the case for Redland's Location 12. Triangle's Location 6 is the nearest point to the receiving array, being only 138m away. This causes a high degree of multipath propagation as the scatterers for the Directions of Departure (DoD) are probably the same as those for the Directions of Arrival (DoA).

The coherence bandwidth, B_{COH}, was evaluated directly from the measured data which is in the frequency domain for a correlation coefficient of 0.9. The following expression was used.

$$\rho(B) = \left| \frac{\sum_{k=1}^{N} \alpha_k \alpha_{k+B}^*}{\sum_{k=1}^{N} \alpha_k \alpha_k^* \sum_{k=1}^{N} \alpha_{k+B} \alpha_{k+B}^*} \right| \qquad (1)$$

$\rho(B)$ is the auto-correlation co-efficient at a lag of B Hz away, N is the number of frequency lines sampled across the bandwidth of the complex channel frequency response and α_k is the amplitude of the k'th frequency line. Figure 8 shows the variation in the coherence bandwidth for the different locations and frequency bands. It should be noted that the value shown at each location was averaged over all 8 receiving elements and 2.2s (400 snapshots) of the measurement period.

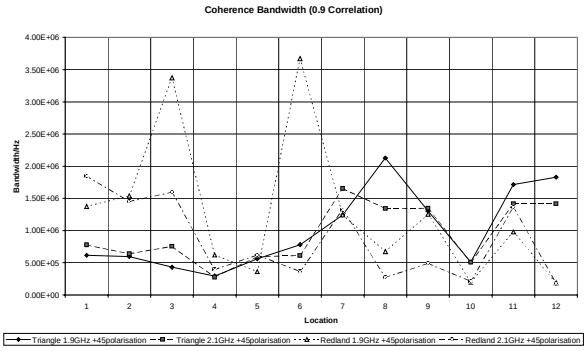

Figure 8: Coherence Bandwidth for +45° Polarisation

The path loss exponent, n, was also evaluated for all the locations from the path loss measured and the propagation distance. The values were averaged over all 8 elements and 2.2s of observation time. It can be seen that the path loss exponent measured is about 3.3 and is fairly constant across the scenarios and frequency bands (Figure 9).

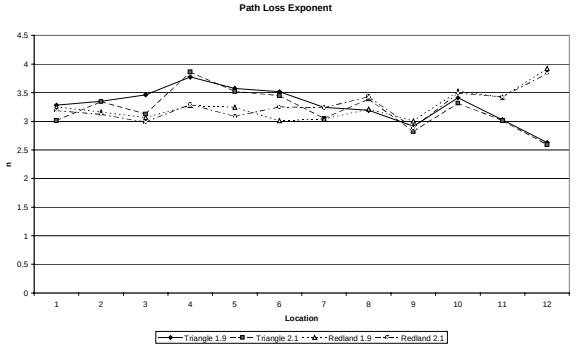

Figure 9: Path Loss Exponent for +45° Polarisation

Temporal correlation, $\rho_{TEMPORAL}$, compares the impulse response of the two frequency bands for each location and gives a measure of the correlation between them. The expression used to evaluate it is similar to (1) but is a cross-correlation between the temporal data in the 1.9GHz band and the 2.1GHz band at zero lag. Figure 10 shows a plot of the variation in the temporal correlation for differing locations in the 2 scenarios. The sub-urban Redland scenario displays a higher degree of correlation in the temporal responses of the two frequency band channels. Triangle's Location 12 shows a particularly high correlation as it is a Line of Sight (LOS) channel. Redland's Location 6 also shows a relatively high degree of correlation as it is on an elevated plane.

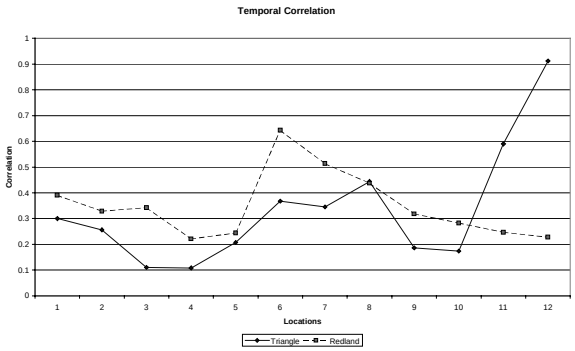

Figure 10: Temporal Correlation for +45° Polarisation

Spatial correlation, $\rho_{SPATIAL}$, is the spatial dual of the temporal correlation. It compares the power azimuth spectra of the two frequency bands and quantifies their degree of likeness. Here again, the Redland scenario exhibits a higher degree of correlation between the two frequency band channels. Figure 11 shows the variations in the spatial correlation.

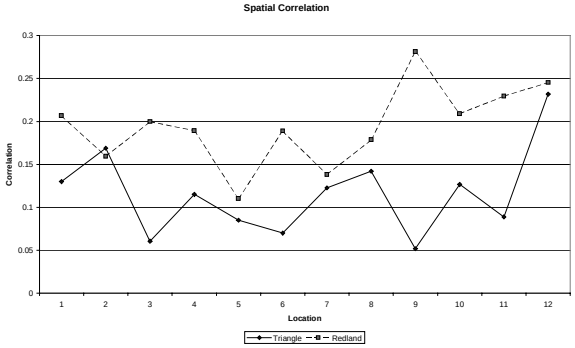

Figure 11: Spatial Correlation for +45° Polarisation

5 CONCLUSIONS

It is observed that the channels which are spaced apart by 200MHz (10% bandwidth spacing at 2GHz) exhibit different responses from both the spatial and temporal domain. However, the differences are slightly more pronounced in the spatial sense with very strong de-correlation and different azimuth spreads. The degree of de-correlation also increases for urban environments, compared to sub-urban settings due to the increased multipath scattering.

This indicates that uplink based downlink beamforming algorithms are sub-optimal when deployed in channels that are multipath rich. Further work is intended to characterise this frequency dependency to enable a robust downlink beamforming scheme.

ACKNOWLEDGEMENTS

The authors gratefully acknowledge financial support of HEFCE for the procurement of the Medav RUSK system under JREI '98, Allgon Systems AB for loan of the UMTS array, Philip Mattos of ST Electronics for the GPS receiver. In addition, we are grateful to the Overseas Research Studentship (ORS) and the University of Bristol for their financial support of S E Foo.

REFERENCES

[1] G Tsoulos, J McGeehan and M Beach, 1997, "Wireless Personal Communications for the 21st Century: European Technologies Advances in Adaptive Antennas", IEEE Communications Magazine, September, pp102-109

[2] 3G Partnership Project Technical Specification, 1999, "UE Radio Transmission and Reception (FDD)", Doc Num TS25.101 v3.1.0

[3] B Allen, J Webber, P Karlsson and M Beach, 2001, "UMTS Spatio-Temporal Propagation Trial Results", IEE ICAP2001, Conference Proceedings No. 480, Vol 2, pp497-501

[4] B Allen, M Beach and P Karlsson, 2001, "Spatial Channel Characterisation of FDD Wireless Links", IEE 3G 2001 Conference

[5] R Thomä, D Hampicke, A Richter, G Sommerkorn, A Schneider, U Trautwein and W Wirnitzer, 2000, "Identification of Time-Variant Directional Mobile Radio Channels" IEEE Trans. Inst & Meas, Vol. 49, pp357-364

[6] G Sommerkorn, D Hampicke, R Klukas, A Richter, A Schneider, R Thomä, 1999, ` Reduction of DOA Estimation Errors Caused by Antenna Array Imperfections", 29th European Microwave Conf, pp282-290

[7] M Haardt, 1996, "Efficient one-, two-, and multidimensional high-resolution array signal processing", PhD. Thesis, ISBN 3-8265-2220-6.

[8] K Pedersen, P Mogensen and B. Fleury, 2000, "A Stochastic Model of the Temporal and Azimuthal Dispersion seen at the Base Station in Outdoor Propagation Environments", IEEE Transactions on Vehicular Technology No. 2, Vol. 49, pp437-447

[9] P Eggers, 1995, "Angular Dispersive Mobile Radio Environments Sensed by Highly Directive Base Station Antennas", IEEE Vehicular Technology Conference Proceedings, pp522-526

[10] P Eggers, 2000, "Comparison of Angular Dispersion Metrices in Synthetic and Measured Radio Channels", AP2000 Conference Proceedings